

Tear Film Stability as a Function of Tunable Mucin Concentration Attached to Supported Lipid Bilayers

Published as part of *The Journal of Physical Chemistry virtual special issue "Stephen G. Boxer Festschrift"*.

Kiara W. Cui, David J. Myung, and Gerald G. Fuller*



Cite This: *J. Phys. Chem. B* 2022, 126, 6338–6344



Read Online

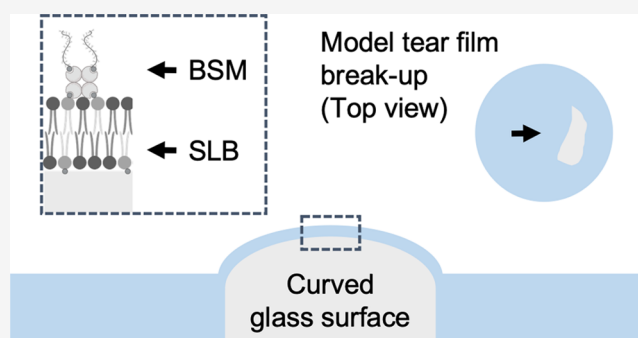
ACCESS |

Metrics & More

Article Recommendations

Supporting Information

ABSTRACT: In this work, we describe the development of a tunable, acellular *in vitro* model of the mucin layer of the human tear film. First, supported lipid bilayers (SLBs) comprised of the phospholipid DOPC (1,2-dioleoyl-*sn*-glycero-3-phosphocholine) and biotinyl cap PE (1,2-dioleoyl-*sn*-glycero-3-phosphoethanolamine-*N*-(cap biotinyl)) are created on the surface of a glass dome with radius of curvature comparable to the human eye. Next, biotinylated bovine submaxillary mucins (BSM) are tethered onto the SLB using streptavidin protein. The mucin presentation can be tuned by altering the concentration of biotinylated BSM, which we confirm using fluorescence microscopy. Due to the optically smooth surface that results, this model is compatible with interferometry for monitoring film thickness. Below a certain level of mucin coverage, we observe short model tear film breakup times, mimicking a deficiency in membrane-associated mucins. In contrast, the breakup time is significantly delayed for SLBs with high mucin coverage. Because no differences in mobility or wettability were observed, we hypothesize that higher mucin coverage provides a thicker hydrated layer that can protect against external disturbances to thin film stability. This advance paves the way for a more physiological, interferometry-based *in vitro* model for investigating tear film breakup.



INTRODUCTION

Flow of a thin fluid film over curved surfaces plays a role in a number of biological and industrial applications, and one such example is in the human eye. A multilayered structure called the tear film comprises the outermost portion of the ocular surface, consisting of an outermost lipid layer and an inner aqueous layer with increasing concentrations of mucins toward the ocular surface.¹ Within the tear film, these high molecular weight glycoproteins called mucins play key roles in maintaining ocular surface health. These biomolecules have protein backbones rich in serine and threonine, providing sites for extensive O-glycosylation that render the ocular surface hydrophilic.²

The two main types of mucins present in the tear film are the secretory mucins (SMs), such as MUC2, MUC5AC, MUC5B, and MUC7, and the membrane-associated mucins (MAMs), such as MUC1, MUC4, and MUC16.³ SMs are present in the tear film aqueous layer and serve functions such as trapping and clearing debris and forming gels that provide lubrication during blinks.² MAMs give antiadhesive character to the corneal epithelial surface² and form a tight protective barrier called the glycocalyx.³ Both types of mucins are thought to contribute to tear film stability by providing shear thinning properties to tears, reducing friction during blinks, capturing

and removing contaminants, acting as a barrier, and enhancing corneal wettability.⁴

Conversely, deficiency of mucins within the tear film can lead to tear film instability.⁴ This instability is a core mechanism behind dry eye disease, a multifactorial ocular pathology affecting hundreds of millions worldwide that is associated with discomfort and blurred vision² as well as inflammation.⁵ Tear film breakup monitored by the introduction of fluorescein to a patient's eye can be used to diagnose dry eye disease in a clinical setting, and different classifications are assigned depending on the timing, location, and shape of tear breakup.⁶ Subsequently, these classifications are used to indicate aqueous deficiency, decreased wettability, or increased evaporation, with possible deficiency of SMs or MAMs tied to each.⁶

Of the methods available to study tear film break up *in vitro*, the Interfacial Dewetting and Drainage Optical Platform (i-

Received: June 15, 2022

Revised: July 25, 2022

Published: August 16, 2022

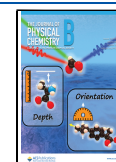


Table 1. Concentrations of Lipids Used for Lipid Vesicle Solutions

lipid	full name	stock concentration	vol lipid/vol DOPC
DOPC	1,2-dioleoyl- <i>sn</i> -glycero-3-phosphocholine (Avanti 850375C)	25 mg/mL	
Biotinyl cap PE	1,2-dioleoyl- <i>sn</i> -glycero-3-phosphoethanolamine-N-(cap biotinyl) (Avanti 870273C)	10 mg/mL	3:40
Fluorescein PE	1,2-dioleoyl- <i>sn</i> -glycero-3-phosphoethanolamine-N-(carboxyfluorescein) (ammonium salt) (Avanti 810332)	1 mg/mL	1:4
Texas Red DHPE	Texas Red 1,2-Dihexadecanoyl- <i>sn</i> -Glycero-3-Phosphoethanolamine, Triethylammonium Salt (Invitrogen T1395MP)	1 mg/mL	9:20

DDrOP) provides the ability to monitor model tear film thickness with respect to space and time using interferometry.⁷ Model tear film breakup is easily assessed by identifying color bands that correspond to film thickness.⁸ Within this system, the lipid layer of the tear film can be mimicked through lipid deposition at the air–liquid interface,⁷ and the aqueous tear film can be mimicked using saline or artificial tear solution.⁹ However, studies performed on the i-DDrOP until now have used dome-shaped surfaces of hydrophilic glass, hydrophobic glass,⁸ or contact lenses⁹ as the substrate, and only incorporation of very thin cells were able to preserve the interferometric capabilities of the system.¹⁰ Culture of corneal epithelial cells on the glass dome, however, disrupted the ability to quantify film thickness.

To enhance the physiological relevance of this platform, we sought to mimic the MAMs of the innermost tear film mucin layer in a way that preserved the capabilities of the i-DDrOP. Supported lipid bilayers (SLBs) are commonly used to mimic the cell membrane due to ease of preparation and stability and can maintain an optically clear path for interferometry.¹¹ Incorporation of membrane-tethered mucins into lipid bilayers has been used as a reductionist system to understand the role of the glycocalyx in preventing infection from pathogens,¹² and here we adapt protocols from immunology to tether biomolecules to supported lipid bilayers.¹³ Using biotinylated phospholipids, biotinylated bovine submaxillary mucins (BSM), and streptavidin protein (sAv), we create SLB-coated glass domes with tunable mucin surface density to mimic various levels of mucin deficiency. We perform experiments to characterize the mucin presentation, lipid mobility, and wettability of these surfaces. Finally, we quantify the effect of mucin presentation on model tear film stability using the i-DDrOP.

METHODS

Preparation of Biotinylated BSM. Monobiotinylated BSM was prepared using the EZ-Link Sulfo-NHS-LC-Biotinylation Kit (Thermo Scientific 21435). To prepare a 10 mg/mL solution of BSM, 10 mg of mucins from bovine submaxillary glands (Sigma M3895) were vortexed then allowed to dissolve overnight in 1 mL of 1X phosphate buffered saline (PBS, Corning 21-040-CV) at 4 °C. Following the instructions from the kit, a 10 mM solution of Sulfo-NHS-LC-Biotin was prepared by dissolving the reagent in ultrapure water (Invitrogen 10977015), and the resulting solution was added to the BSM solution in a 20-fold molar excess. This biotin labeling reaction was allowed to proceed at 4 °C for 2 h, after which excess unreacted biotin reagent was removed using a desalting column. To confirm that the BSM molecules were monobiotinylated, a HABA assay was performed on the purified protein solution to estimate biotin incorporation. The final protein solution was aliquoted and stored at –20 °C until use.

Preparation of Lipid Vesicle Solutions for SLBs. To generate lipid vesicle solutions, volumes of stock lipid solutions were combined according to Table 1. Stock solutions were stored in chloroform in glass vials capped with Teflon mini-nerst valves (Sigma 33300) and transferred using a 50 μ L Hamilton syringe. All experimental conditions included DOPC, conditions involving tethering of mucins included biotinyl cap PE, and fluorescent imaging experiments incorporated either Texas Red DHPE or fluorescein PE.

Chloroform was removed from the combined lipid solution using a gentle stream of compressed air until only lipid remained. The lipids were then resuspended in PBS to a final concentration of 1 mg/mL DOPC then allowed to spontaneously form large unilamellar vesicles at 4 °C for 2 h and up to overnight. Conditions using fluorescent lipids were shielded from light using aluminum foil. The large unilamellar vesicle solution was passed through an extruder containing a 0.1 μ m pore size polycarbonate membrane (Avanti 610000), generating smaller vesicles in solution. Finally, this solution was diluted with two-fold its volume using PBS for a final DOPC concentration of 0.33 mg/mL.

Thin Film Stability Experiments Using Mucin-Coated SLBs on Curved Glass Substrates. To study the stability of thin liquid films on a curved SLB and mucin-coated substrate, the i-DDrOP system was used. Full details of the setup can be found in a previous report.⁸ Briefly, this interferometry-based instrument consists of a Teflon Langmuir trough through which a platform connected to a motorized stage runs. The system can be heated and kept at physiological temperature (37 °C) via a PID controller and thermocouple setup. The trough is filled with PBS, and a glass dome whose radius of curvature mimics that of the adult human eye (7.9 mm) is placed atop the platform and submerged. Following heating of the trough contents, raising the apex of the dome 1 mm above the air–liquid interface captures a thin liquid film of comparable thickness to the human tear film (several microns). The stability of this thin film is monitored using an overhead camera and diffuse light source until film breakup occurs. The setup is shielded from ambient air flow while still allowing for evaporation. The ambient humidity remains around 30–35%.

To prepare mucin-coated supported lipid bilayers on a curved substrate for i-DDrOP experiments, plano-convex UV-fused silica domes (Lattice Electro Optics UF-PX-10-15) were first precleaned using 2% Hellmanex III (Hellma Analytics) in Milli-Q water, Milli-Q water, ethanol, acetone, and Milli-Q water again. A clean surface for lipid deposition was ensured by performing an i-DDrOP experiment with Milli-Q water at room temperature, and only domes that did not exhibit irregular, nonconcentric breakup were used. Clean domes were stored in 3 mL of PBS in individual wells of a 12-well plate (Corning 3513) until deposition.

To deposit SLBs onto the domes, 2.5–3 mL of lipid vesicle solution was added to a well in a 12-well plate for each dome,

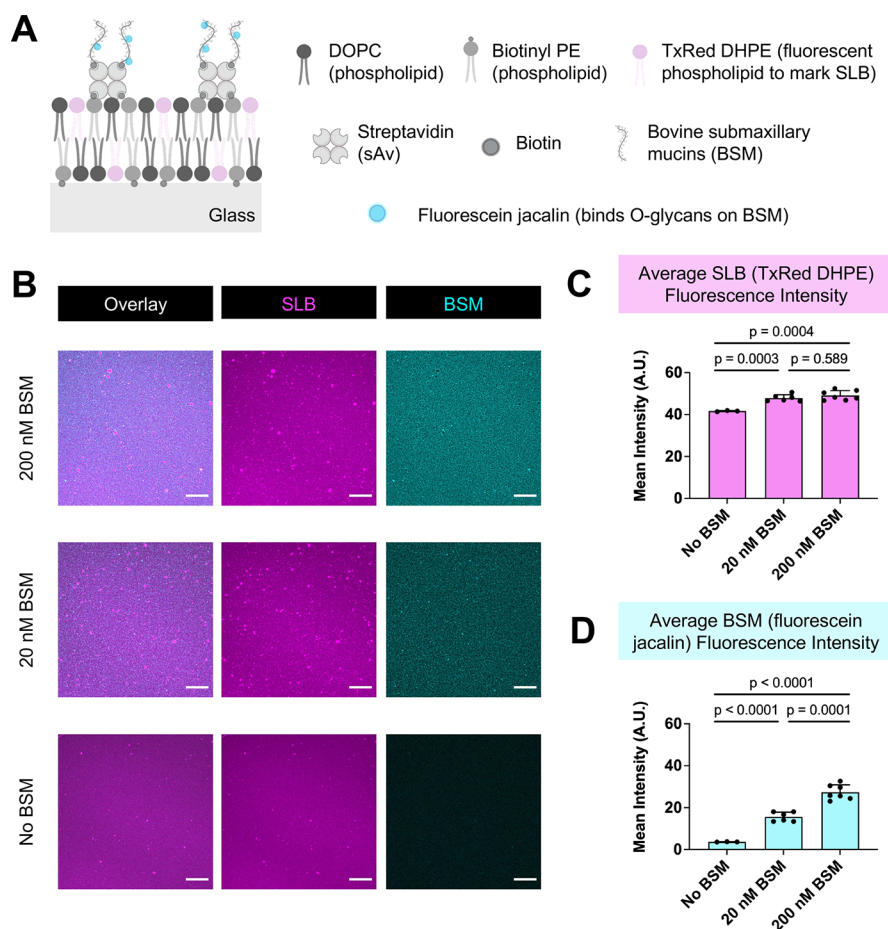


Figure 1. Tunable presentation of mucins on supported lipid bilayers (SLBs). (A) Composition of mucin-tethered SLBs, including fluorescent tags for imaging. (B) Confocal microscopy images showing the SLB (magenta), BSM (cyan), and overlay for various levels of BSM tethering. Scale bar, 20 μm . (C) Average fluorescence intensity of TxRed DHPE, marking the SLB, for conditions in (B). Data are mean \pm SD, significance represents a Brown-Forsythe and Welch's ANOVA test. (D) Average fluorescence intensity of fluorescein jacalin, marking BSM, for conditions in (B). Data are mean \pm SD, significance represents a Brown-Forsythe and Welch's ANOVA test.

then the dome was transferred into that solution and allowed to incubate at room temperature for 30 min. To rinse off excess vesicles after this time, each SLB-coated dome was gently dipped in and out of three wells filled with 2 mL PBS each.

To attach mucins to SLBs containing biotinyl PE, solutions containing monobiotinylated BSM bound to streptavidin were prepared using a protocol adapted from Crites et al.¹³ Purified, lyophilized streptavidin protein (ThermoFisher 21122) was reconstituted in PBS to form a 1 mg/mL solution. To create a 2 μM BSM complex solution, equal volumes of a 2 mg/mL solution of monobiotinylated BSM in PBS and a 0.424 mg/mL solution of streptavidin in PBS were mixed and allowed to react for at least 10 min at room temperature. Dilutions to 200 nM, 100 nM, and 20 nM were done using PBS. Biotinyl SLB-coated domes were then added to wells containing 2.5 mL each of the BSM complex solution and incubated for 45 min at room temperature. To rinse off excess reagent, each SLB-coated dome was gently dipped in and out of three wells filled with 2 mL PBS each.

For each i-DDrOP experiment, SLB and mucin-coated domes were submerged in 20 mL of PBS within the trough, and the PBS was heated to 37°C for 15 min. PBS adjusted to the pH of the eye (7.9) using 0.1 M NaOH was used. Videos monitoring thin film stability were recorded at 20 fps until film

breakup. Custom-built software in MATLAB was used to add timestamps to the videos. The point at which stage motion stopped after the dome was raised was assigned to be $t = 0$, and tear breakup time (TBUT) was assigned to the first instance of sudden dewetting at which the film thickness dropped to the first interferometric color band (approximately 50 nm, see Figure 3). Graphs were made and statistical analysis was done using Prism 9.

Epifluorescence Microscopy. To assess the deposition of SLBs on the glass domes, lipid vesicles consisting of DOPC and fluorescein PE were deposited onto domes as for an i-DDrOP experiment. Domes remained submerged in PBS in a 6 cm Petri dish during imaging. The 10 \times objective of an upright Zeiss AxioImager widefield microscope was used to capture tiled images, which were then stitched together using Zeiss Zen software. Because the glass dome may alter the optical path of the imaging laser, goggles protecting against 488 nm light were worn throughout.

Fluorescence Confocal Microscopy. To visualize the mucin presentation on the surface of the SLBs, the preparation protocol for glass domes was adapted to 96-well glass bottom plates for fluorescence confocal microscopy. Glass bottom wells were cleaned with 200 μL of each solution as above, with the exception of acetone as it is not compatible with plastic. To deposit SLBs, 100 μL of lipid vesicle solution containing Texas

Red DHPE was added to each well for 30 min at room temperature. Excess vesicles were gently removed by adding and removing 250 μL of PBS three times. To each well, 100 μL of BSM complex solution were added and allowed to incubate at room temperature for 45 min. A negative control was performed by adding PBS rather than BSM complex solution. Excess reagent was gently removed by adding and removing 250 μL of PBS three times. To label the mucins, 100 μL of 1:500 fluorescein jacalin (Vector Laboratories FL-1151) were added to each well and incubated at room temperature for 20 min. Finally, excess reagent was gently removed by adding and removing 250 μL of PBS three times. Samples were imaged using a 63 \times oil objective on an inverted confocal microscope (Zeiss LSM780), and average intensities were measured using Fiji.

Fluorescence Recovery after Photobleaching (FRAP).

To quantify the fluidity of the SLBs on the glass substrate, SLB deposition was performed as for confocal microscopy using a lipid vesicle solution containing fluorescein PE. FRAP was performed by taking images on the confocal microscope using a 63 \times oil objective every 0.5 s for a total of 1 min, and a circular region of diameter 6.39 μM was bleached at 100% laser power after 20 frames. Normalization to account for sample-to-sample variation as well as intrinsic photobleaching was performed in Fiji using macros from the Stowers Institute, and data was further processed using custom software built in MATLAB. Postbleach curves were fitted to eq 1, where I is the normalized intensity, a is the mobile fraction, and b is the time constant. Diffusion coefficients were calculated according to eq 2, assuming a Gaussian bleach laser profile and where r_n is the bleach region radius.¹⁴

$$I = a(1 - e^{-bt}) \quad (1)$$

$$D = \frac{r_n^2}{4t_{1/2}}, \quad t_{1/2} = \frac{\ln 2}{b} \quad (2)$$

Wettability Measurements. To understand the wettability of the various conditions tested using the i-DDrOP, measurements were performed on flat glass substrates using a contact angle goniometer (Rame-Hart 290). Rather than glass domes, small pieces of a glass coverslip, cut using a diamond-tipped pen, were used to prepare mucin-coated SLBs as for the i-DDrOP experiments. To replicate drainage on the i-DDrOP and avoid confounding effects from removal of samples from PBS, samples were allowed to dry, or were blotted dry from the edge, until no liquid was visible. A 3–5 μL drop of pH 7.9 PBS was added to each substrate and videos documenting drop spreading were recorded at 30.3 fps.

RESULTS

Tunable Mucin Density on SLB-Coated Surfaces. To verify that our methods were capable of depositing supported lipid bilayers on curved glass surfaces, we first performed a number of imaging experiments. Widefield fluorescence imaging showed successful deposition of SLBs on glass domes with no discernible gaps in coverage (Figure S1). Due to the distortion of the optical path and challenges of performing microscopy on curved surfaces, we performed subsequent experiments on flat glass prepared using the same cleaning protocols.

To understand differences in mucin coverage on the SLBs, we incubated SLBs containing biotinyl PE with varying

concentrations (0, 20, or 200 nM) of biotinylated BSM complex solution. We then used Texas Red DHPE to label the SLBs and fluorescein jacalin to label mucins for fluorescence confocal microscopy (Figure 1A). This procedure resulted in comparable levels of SLB deposition with varying levels of BSM tethering to the SLB surface (Figure 1B). Quantifying the average fluorescence intensity of TxRed DHPE, marking the SLB, we found no statistically significant difference between the 20 nM and 200 nM BSM conditions ($p = 0.589$, Figure 1C). Both differed from the no-BSM condition ($p = 0.0003$, 0.0004), which likely displayed a lower mean intensity due to fewer bright puncta (Figure 1B, C). Imaging of the SLB with unlabeled mucins over the 45 min incubation period revealed a slight growth in size of these puncta in the initial 5 min period but none thereafter (Figure S2). Because these puncta are only present in the TxRed channel, it suggests that addition of BSM to the SLB results in clustering of the TxRed DHPE lipid molecules. In contrast, quantification of the mean fluorescence intensity of fluorescein jacalin, which binds the O-glycans on BSM, showed that incubation with an increasing concentration of BSM increased mucin tethering onto SLBs in a statistically significant manner ($p \leq 0.0001$, Figure 1D). In all cases, the fluorescent signal is confined to a narrow plane in z -axis, as expected.

Mobility and Wettability of Mucin-Covered SLBs. We quantified the effect of various components of the mucin-tethered SLBs on lipid mobility on the glass surfaces using FRAP (Figure S3A). Comparing SLBs comprised of only DOPC, DOPC and biotinyl PE, and DOPC/biotinyl PE with tethered BSM, we found that neither the mobile fraction nor the diffusion coefficient changed significantly between the three conditions (Figure S3B). A mobile fraction around 0.8 in all cases indicated that the SLBs were fluid on the glass surface, and the diffusion coefficient was measured to be approximately 1.0×10^{-12} m^2/s . Both values are lower but comparable to those reported in previous literature using DOPC SLBs, perhaps due to differences in the fluorescent lipids used and surface preparation.¹⁵

Measurements using the sessile drop contact angle method indicated that all surface preparations (0, 20, 200 nM BSM on SLBs) were highly hydrophilic. Upon contact with the surfaces, the drop of PBS spread fully until no contact angle was observed in all cases (Figure 2). No discernible differences in wettability of the three surfaces were observed.

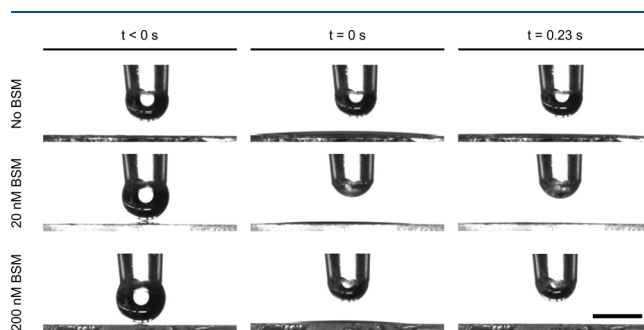


Figure 2. Effect of increased mucin presentation on wettability. Images from sessile drop contact angle experiments showing the frame right before the drop contacts the surface ($t < 0$ s), the frame at which the drop contacts the surface ($t = 0$ s), and $t = 0.23$ s after contact with the surface for various densities of tethered mucins on SLBs. Scale bar, 1 mm.

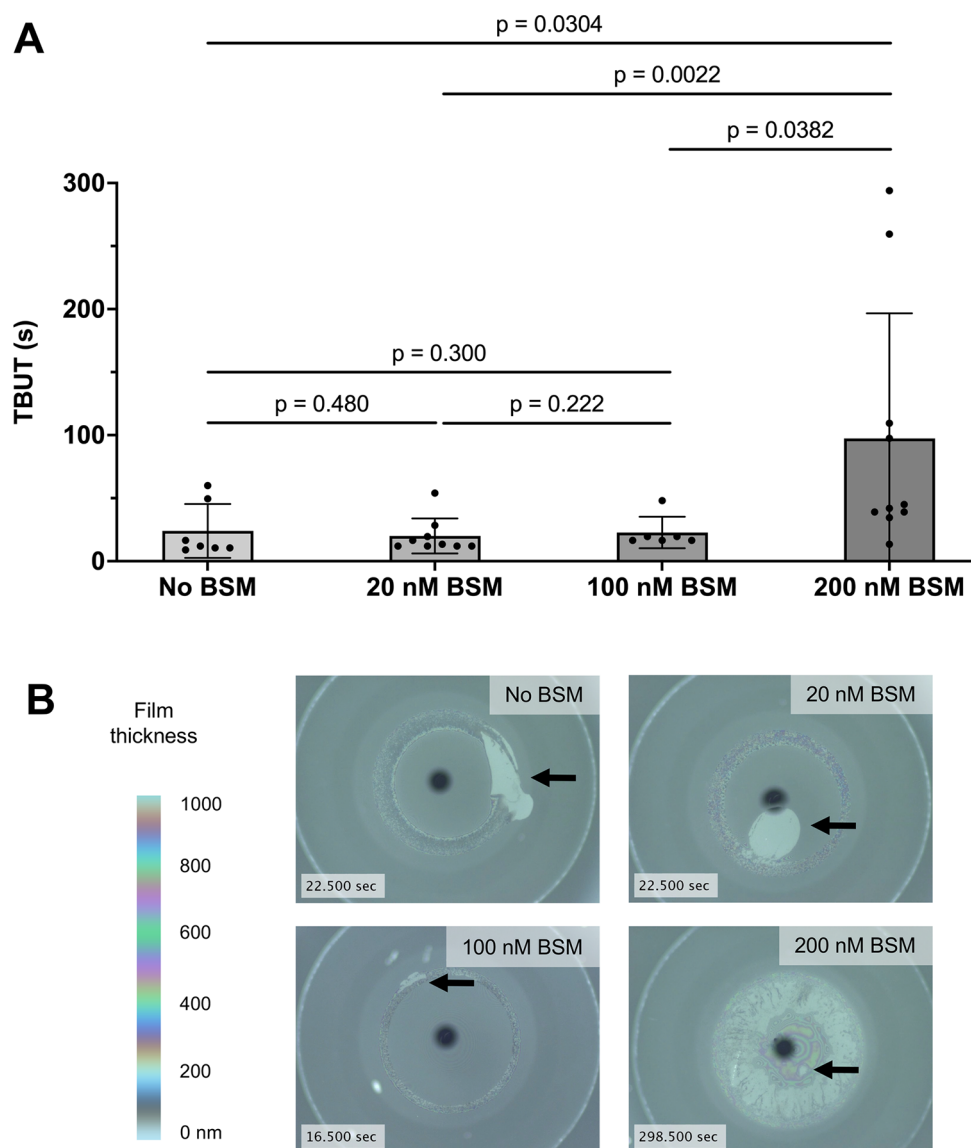


Figure 3. Effect of increased mucin presentation on model tear film breakup time (TBUT). (A) TBUT as a function of mucin presentation. Data are mean \pm SD, significance represents a Mann–Whitney rank sum test. (B) Representative time points for model tear film breakup for various levels of mucin presentation. Black arrow indicates site of observed dewetting, and color map indicates film thicknesses in nm.

Tear Film Breakup in the Presence of Varying Mucin Presentation. We next measured the stability of thin PBS films on mucin-tethered SLBs deposited on glass domes to mimic breakup of the human aqueous tear film. To do so, i-DDrOP experiments were performed for SLBs incubated with 0, 20, and 200 nM BSM. We also incorporated a condition incubated with 100 nM BSM to better understand the concentration dependence of our system. We found that the average tear breakup times (TBUT) for the 0 nM, 20 nM, and 100 nM BSM conditions were 24.0, 20.0, and 22.8 s, respectively, with no statistically significant difference (Figure 3A). Breakup for these films occurred suddenly as a single location, often near the edge where the film thins first, due to the curvature of the dome (Figure 3B). In addition, the film thickness in the breakup region dropped from over 1000 to 50 nm or less at the TBUT. Though the TBUT's were similar, the area of the initial breakup region was notably smaller for the 100 nM BSM condition as compared to the 0 nM and 20 nM conditions. Following the TBUT, the thin film generally

continued to decline in thickness, and the region of breakup continued to expand (Video S1A–C). Oscillations in thickness were observed as well, likely due to evaporation-driven Marangoni flows.⁸ Experiments with SLBs comprised of DOPC alone (no biotinyl PE) behaved similarly (SI Video 1E). In contrast, the average TBUT for the 200 nM BSM condition was significantly higher at 97.4 s ($p = 0.0304, 0.0022, 0.0382$) than the 0 nM, 20 nM, and 100 nM BSM conditions, respectively. The variability in these data were also higher (Figure 3A,B). Because the TBUT was delayed, breakup occurred at locations with smaller film thicknesses of several hundred nanometers. Throughout the measurement period, the outer edges of these films oscillated when the thicknesses decreased below 100 nm, indicated by the rapid color changes between the dome edge and thicker regions (SI Video 1D). Fewer color changes were seen at the regions of breakup for the 0 nM, 20 nM, and 100 nM BSM conditions, suggesting that the liquid film was thinner and remained below 50 nm in thickness.

DISCUSSION

In this study, we developed a protocol to create SLBs with varying levels of mucin presentation, enabling the study of thin liquid film stability on a curved substrate mimicking the membrane-associated mucins of the ocular tear film. Such a system allowed us to generate varying surface concentrations of mucins as a way to model mucin-deficient dry eye disease.⁴ Our results suggest that mucin presentation in our acellular *in vitro* model can be tuned simply by incubation with different concentrations of biotinylated BSM and streptavidin complex. While methods have been successfully developed to tune mucin presentation on corneal epithelial cells,¹⁶ our method ensures compatibility with interferometry on the i-DDrOP by maintaining an optically smooth surface. This feature enables us to monitor the thickness of the liquid film over time on a curved substrate. We imagine that the system is compatible with both studies of how biomolecules or therapeutics within the tear film interact with mucins, as well as further studies of thin film fluid dynamics on surfaces of varying curvature coated with supported lipid bilayers.

Of the mucins present within the tear film, our system most closely mimics the membrane associated mucins (MAMs) rather than the secretory mucins. From a physical chemistry perspective, the roles of these membrane associated mucins such as MUC1, 4, and 16 include comprising a hydrophilic glycocalyx to promote wettability of the ocular surface and serving as a barrier against debris and pathogens.³ We note that in our study we use bovine submaxillary mucins (BSM) as a commercially available and economical reagent, though the same chemistry can be readily applied to other mucins. BSM is commonly used as a source of the secretory mucin MUC5B,¹⁷ but it exhibits high degrees of O-glycosylation and a comparable molecular weight to MUC1 and MUC4.³ Our platform is also adaptable to combinations of several mucins by exposure to a mixture during the mucin incubation step.

While we observed few changes in the randomly distributed sites marked by TxRed DHPE within the SLB (Figure S2), further changes in aggregation and film morphology may occur over time. In our study, any changes that occurred between the creation of the surface and measurement on the i-DDrOP were minor enough such that the modified bilayer surfaces remained wettable and optically smooth through the point of measurement. Whether the surface properties change over longer periods of time and if such behavior impacts tear film stability may be an interesting topic for future studies.

Though the data resulting from our system can be quantified in various ways, we chose to quantify the TBUT as it is the predominant metric used to assess tear film stability clinically.⁶ Our results indicate that a higher degree of mucin presentation on the SLB surface resulted in a significant delay in tear breakup time. While the lower degrees of mucin presentation, 20 nM and 100 nM, yielded comparable TBUT's to having no tethered mucins, the intermediate coverage of 100 nM BSM was able to decrease the area of the breakup. This result suggests the potential for a concentration-dependent response, and an interesting future avenue would be to understand the TBUT response for a wider range of mucin densities. When compared to a tear-film oriented clinical diagnosis, the tear breakup patterns we observe in the lower density and no-mucin conditions are most reminiscent of a "line break" or "dimple break".⁵ These breakup patterns occur during or after tear movement, analogous to the liquid movement observed

during an i-DDrOP experiment and are thought to be due to aqueous deficiency and decreased wettability, respectively.⁵ For the high mucin coverage conditions, delayed breakup is most reminiscent of the "random break" that occurs after tear movement has stopped, which is thought to be due to tear thinning from evaporation.⁵ Given that aqueous deficiency is not a factor in our study and that mucin density appeared to have no impact on the wettability of our surfaces (Figure 2), we hypothesize that a higher mucin density is able to maintain a more substantial hydration layer that protects against spontaneous dewetting and that a certain threshold of mucin density is needed to achieve this effect. Our interferometry measurements indicate that the higher mucin presentation is able to maintain a higher film thickness up to around 100 nm after film thinning at the periphery, and the antiadhesive properties of the tethered mucins may contribute to removal of debris capable of inducing breakup as well.¹⁸ For comparison, the glycocalyx formed by the membrane-associated mucins is thought to be 200–500 nm in thickness and also incorporates the largest MAM, MUC16.³ This interpretation is also consistent with the higher variability we observe in TBUT in that high mucin presentation cannot fully preclude a short breakup time due to debris and inhomogeneity on the surface, but the average TBUT increases.

We note that our approach allows us to isolate and control the presentation of membrane associated mucins to understand their effect on model tear film stability. The human eye, as well as *in vitro* models that incorporate cells, are subject to more factors including the presence of additional biomolecules and tear film components, cell signaling, movement, blinking, and gravity oriented in a different direction. Cell-based models also have the additional features of surface roughness that affect wettability,¹⁶ which render interferometry-based measurements more difficult. We also emphasize that our interpretation relies on the ability to distinguish film thickness through interferometry and that more advanced techniques such as hyperspectral imaging may be incorporated to more robustly quantify film thicknesses.¹⁹ Further, we anticipate that the incorporation of additional tear film components such as secretory mucins will delay the TBUT as the presence of secretory mucins is thought to serve as a protective barrier and clear pathogens.² Incorporation of the outermost lipid layer of the tear film should also increase model tear film stability, as was shown in previous i-DDrOP studies focusing on this component.⁷ Nevertheless, our study offers a protocol that does not require cell culture and is able to isolate the effect of membrane associated mucins on tear film stability *in vitro*. Notably, the procedures we describe here enhance the physiological relevance of the model ocular surface in the i-DDrOP setting, which is already capable of mimicking the aqueous and lipid components of the tear film.⁷ Thus, these components together create a more complete *in vitro* model of the tear film, and this advance will be useful in future studies of tear film stability and flow over curved substrates.

CONCLUSIONS

In summary, we have developed a method for tuning mucin presentation on supported lipid bilayer-coated curved glass substrates through biotin–streptavidin coupling. This method allows us to mimic the membrane-associated mucins present in the human tear film on the Interfacial Dewetting and Drainage Optical Platform, or i-DDrOP. This interferometry-based instrument is able to monitor film thickness and stability,

and we found that higher mucin presentation is able to delay the observed tear film breakup time. This method creates a more physiologically relevant, convex *in vitro* platform to understand factors that affect tear film stability.

■ ASSOCIATED CONTENT

SI Supporting Information

The Supporting Information is available free of charge at <https://pubs.acs.org/doi/10.1021/acs.jpcb.2c04154>.

Additional experimental images and data describing SLB and BSM deposition and FRAP (PDF)

Representative videos of TBUT (MP4)

■ AUTHOR INFORMATION

Corresponding Author

Gerald G. Fuller – Department of Chemical Engineering, Stanford University, Stanford, California 94305, United States; orcid.org/0000-0002-2924-053X; Email: gfg@stanford.edu

Authors

Kiara W. Cui – Department of Chemical Engineering, Stanford University, Stanford, California 94305, United States

David J. Myung – Department of Chemical Engineering, Stanford University, Stanford, California 94305, United States; Byers Eye Institute at the School of Medicine, Stanford, California 94305, United States

Complete contact information is available at: <https://pubs.acs.org/doi/10.1021/acs.jpcb.2c04154>

Notes

The authors declare no competing financial interest.

■ ACKNOWLEDGMENTS

We thank V. Xia, C. Liu, E. de la Serna, and V. Vachharajani for discussion. Confocal microscopy was performed in the Stanford Cell Sciences Imaging Facility (CSIF). Part of this work was performed at the Stanford Nano Shared Facilities (SNSF), supported by the National Science Foundation under award ECCS-1542152. Schematics in Figure 1 and Figure S1 were made using BioRender, and all plots were created in Prism 9. K.W.C. is supported by the Stanford EDGE, Bio-X Bowes, and ChEM-H CBI fellowships and National Institutes of Health (NIH) Grant T32GM120007. D.M. is supported by the NIH (National Eye Institute K08EY028176 and a Departmental P30-EY026877 core grant), as well as a core grant and Career Development Award from Research to Prevent Blindness (RPB).

■ REFERENCES

- (1) Craig, J. P.; Nichols, K. K.; Akpek, E. K.; Caffery, B.; Dua, H. S.; Joo, C.-K.; Liu, Z.; Nelson, J. D.; Nichols, J. J.; Tsubota, K.; et al. TFOS DEWS II definition and classification report. *Ocul. Surf.* **2017**, *15*, 276–283.
- (2) Mantelli, F.; Argüeso, P. Functions of ocular surface mucins in health and disease. *Curr. Opin. Allergy Clin. Immunol.* **2008**, *8*, 477.
- (3) Ablamowicz, A. F.; Nichols, J. J. Ocular surface membrane-associated mucins. *Ocul. Surf.* **2016**, *14*, 331–341.
- (4) Georgiev, G. A.; Eftimov, P.; Yokoi, N. Contribution of mucins towards the physical properties of the tear film: a modern update. *Int. J. Mol. Sci.* **2019**, *20*, 6132.
- (5) Kojima, T.; Dogru, M.; Kawashima, M.; Nakamura, S.; Tsubota, K. Advances in the diagnosis and treatment of dry eye. *Prog. Retinal Eye Res.* **2020**, *78*, 100842.
- (6) Yokoi, N.; Georgiev, G. A. Tear film-oriented diagnosis and tear film-oriented therapy for dry eye based on tear film dynamics. *Invest. Ophthalmol. Visual Sci.* **2018**, *59*, DES13–DES22.
- (7) Bhamla, M. S.; Nash, W. L.; Elliott, S.; Fuller, G. G. Influence of lipid coatings on surface wettability characteristics of silicone hydrogels. *Langmuir* **2015**, *31*, 3820–3828.
- (8) Rabiah, N. I.; Sato, Y.; Kannan, A.; Kress, W.; Straube, F.; Fuller, G. G. Understanding the adsorption and potential tear film stability properties of recombinant human lubricin and bovine submaxillary mucins in an *in vitro* tear film model. *Colloids Surf., B* **2020**, *195*, 111257.
- (9) Suja, V. C.; Verma, A.; Mossige, E.; Cui, K.; Xia, V.; Zhang, Y.; Sinha, D.; Joslin, S.; Fuller, G. G. Dewetting characteristics of contact lenses coated with wetting agents. *J. Colloid Interface Sci.* **2022**.
- (10) Hermans, E.; Saad Bhamla, M.; Kao, P.; Fuller, G. G.; Vermant, J. Lung surfactants and different contributions to thin film stability. *Soft Matter* **2015**, *11*, 8048–8057.
- (11) Chan, Y.-H. M.; Boxer, S. G. Model membrane systems and their applications. *Curr. Opin. Chem. Biol.* **2007**, *11*, S81–S87.
- (12) Delaveris, C. S.; Webster, E. R.; Banik, S. M.; Boxer, S. G.; Bertozzi, C. R. Membrane-tethered mucin-like polypeptides sterically inhibit binding and slow fusion kinetics of influenza A virus. *Proc. Natl. Acad. Sci. U. S. A.* **2020**, *117*, 12643–12650.
- (13) Crites, T. J.; Maddox, M.; Padhan, K.; Muller, J.; Eigsti, C.; Varma, R. Supported lipid bilayer technology for the study of cellular interfaces. *Curr. Protoc. Cell Biol.* **2015**, *68*, 24–5.
- (14) Kang, M.; Day, C. A.; Kenworthy, A. K.; DiBenedetto, E. Simplified equation to extract diffusion coefficients from confocal FRAP data. *Traffic* **2012**, *13*, 1589–1600.
- (15) Pincet, F.; Adrien, V.; Yang, R.; Delacotte, J.; Rothman, J. E.; Urbach, W.; Tareste, D. FRAP to characterize molecular diffusion and interaction in various membrane environments. *PLoS One* **2016**, *11*, No. e0158457.
- (16) Liu, C.; Madl, A. C.; Cirera-Salinas, D.; Kress, W.; Straube, F.; Myung, D.; Fuller, G. G. Mucin-like glycoproteins modulate interfacial properties of a mimetic ocular epithelial surface. *Adv. Sci.* **2021**, *8*, 2100841.
- (17) Song, D.; Iverson, E.; Kaler, L.; Bader, S.; Scull, M. A.; Duncan, G. A. Modeling airway dysfunction in asthma using synthetic mucus biomaterials. *ACS Biomater. Sci. Eng.* **2021**, *7*, 2723–2733.
- (18) Sumiyoshi, M.; Ricciuto, J.; Tisdale, A.; Gipson, I. K.; Mantelli, F.; Argüeso, P. Antiadhesive character of mucin O-glycans at the apical surface of corneal epithelial cells. *Invest. Ophthalmol. Visual Sci.* **2008**, *49*, 197–203.
- (19) Chandran Suja, V.; Sentmanat, J.; Hofmann, G.; Scales, C.; Fuller, G. G. Hyperspectral imaging for dynamic thin film interferometry. *Sci. Rep.* **2020**, *10*, 1–8.